

**Resveratrol Inhibition of Rac1-Derived Reactive Oxygen Species by AMPK Decreases
Blood Pressure in a Fructose-Induced Rat Model of Hypertension**

Pei-Wen Cheng, PhD^{1,2}; Hui-Chieh Lee, MD³; Pei-Jung Lu, PhD⁴; Hsin-Hung Chen, MS^{1,5};
Chi-Cheng Lai, MD⁶; Gwo- Ching Sun, MD, PhD⁷; Tung-Chen Yeh, MD, PhD⁶; Michael
Hsiao, DVM, PhD⁸; Yu-Te Lin, MD, PhD⁹; Chun-Peng Liu, MD⁶; Ching-Jiunn Tseng, MD,
PhD^{1,5, 10,11}

¹Department of Medical Education and Research, Kaohsiung Veterans General Hospital, Kaohsiung, Taiwan; ²Yuh-Ing Junior College of Health Care & Management, Kaohsiung, Taiwan; ³Department of Diving Medicine, Zouying Branch of Kaohsiung Armed Forces General Hospital Kaohsiung, Taiwan; ⁴Institute of Clinical Medicine, National Cheng-Kung University, Tainan, Taiwan; ⁵Institute of Clinical Medicine, National Yang-Ming University, Taipei, Taiwan; ⁶Department of Internal Medicine, Division of Cardiology, Kaohsiung Veterans General Hospital, Kaohsiung, Taiwan; ⁷Department of Anesthesiology, Kaohsiung Medical University Hospital, Kaohsiung Medical University, Kaohsiung, Taiwan; ⁸Genomics Research Center, Academia Sinica, Taipei, Taiwan; ⁹Section of Neurology, Kaohsiung Veterans General Hospital, Taiwan; ¹⁰Department of Pharmacology, National Defense Medical Center, Taipei, Taiwan; ¹¹Department of Medical Research, China Medical University Hospital, China Medical University, Taichung 40402, Taiwan

Correspondence:

Ching-Jiunn Tseng, MD, PhD

Department of Medical Education and Research, Kaohsiung Veterans General Hospital, 386
Ta-Chung 1st Rd., Kaohsiung, Taiwan 813

E-mail: cjtseng@vghks.gov.tw

Tel: 886-7-3422121 ext. 1505; Fax: 886-7-3468056

or

Chun-Peng Liu, MD

Department of Administration, Kaohsiung Veterans General Hospital, Kaohsiung, Taiwan

E-mail:

cpliu@vghks.gov.tw

Telephone: 886-7-3422121ext. 2011

Pei-Wen Cheng and Hui-Chieh Lee contributed equally to this work.

Running title: AMPK Inactivates Fructose-Induced NADPH oxidase

Supplement Method

ROS production in the RVLM

The endogenous in vivo ROS produced in the RVLM was determined by staining RVLM slices with 2',7'-dichlorofluorescein (H2DCF) (Sigma Chemical Co., St. Louis, MO, USA). The RVLM dissected out of the studied rats was placed in OCT compound (Shandon Cryomatrix; Thermo Electron Co., Pittsburgh, PA), flash-frozen in a methylbutane-chilled bath, and then placed in liquid nitrogen. Cryostat slices (10 μ m) were stained in the dark for 30 min at 37 °C in a humidified 5% CO₂ incubator with 10 μ M H2DCF. The samples were analyzed using fluorescence microscopy and Zeiss LSM Image software (Carl Zeiss MicroImaging, Jena, Germany).

Supplement Figure

Supplement figure 1. Cross section of the medulla oblongata rostral to the obex, indicating the location of the RVLM.

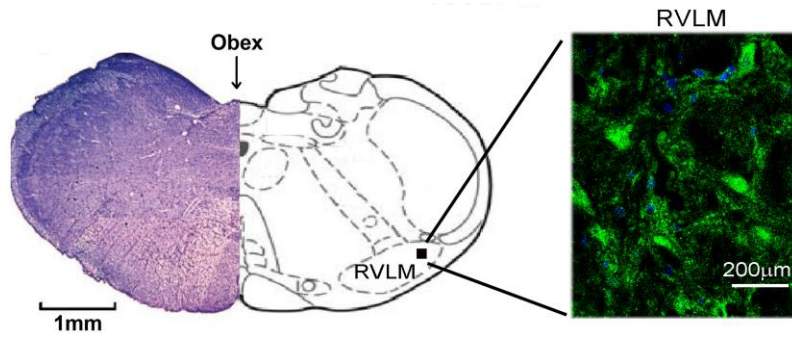
Supplement figure 2. Resveratrol abolish the ROS generation in the RVLM of rats with fructose-induced hypertension. Confocal microscopy analysis of green fluorescence was used to estimate ROS levels in the RVLM after treatment with resveratrol. The representative images shown demonstrate that the elevation of the ROS level was significantly decreased in the RVLM after treatment with resveratrol. The images were photographed at \times 400 magnification. We examined 4 groups (control; 10% fructose-treated; 10% fructose+resveratrol and 10% fructose+resveratrol+compound C; n=6 for each). The values shown are the means \pm SEM, n=6. *P<0.05, **P<0.01. Scale bar: 20 μ m.

Supplement figure 3. Full Western blots and fluorescent gel scans. Red boxes indicate regions cropped for main figure 2B-C.

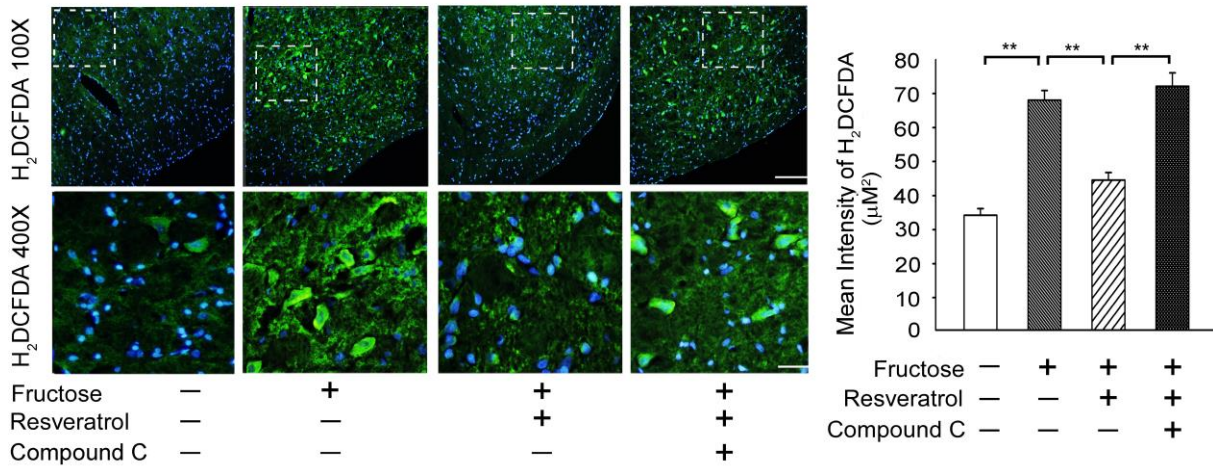
Supplement figure 4. Full Western blots and fluorescent gel scans. Red boxes indicate regions cropped for main figure 3F-G.

Supplement figure 5. Full Western blots and fluorescent gel scans. Red boxes indicate regions cropped for main figure 4A-B.

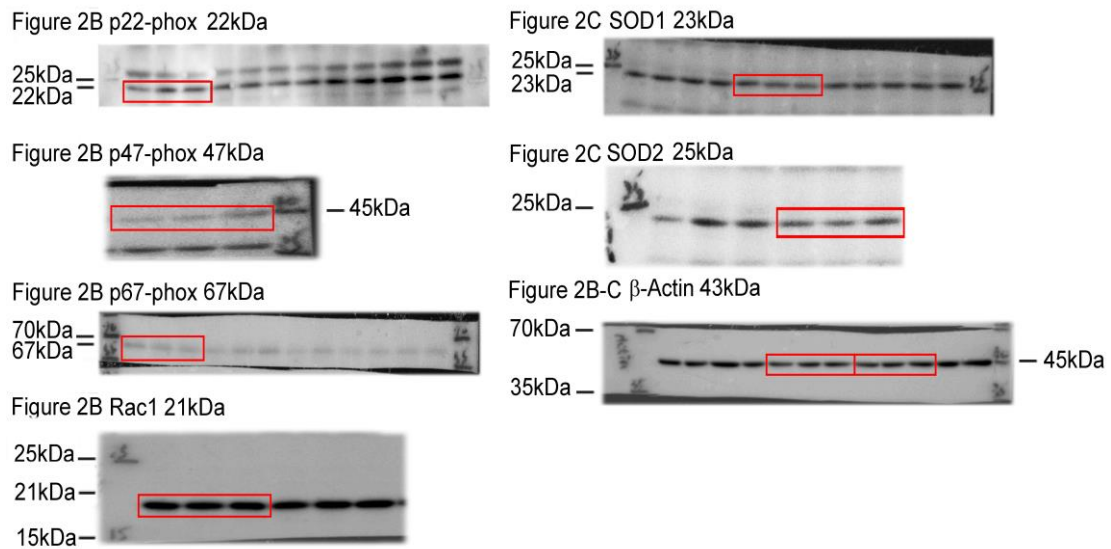
Supplement figure 1.



Supplement figure 2.



Supplement figure 3.



Supplement figure 4.

Figure 3F P-ACC^{S79} 280kDa

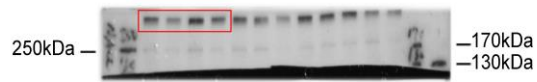


Figure 3G p22-phox 22kDa

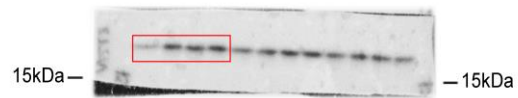


Figure 3F P-AMPK^{T172} 62kDa

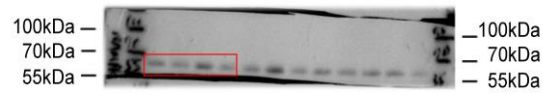


Figure 3G SOD2 25kDa

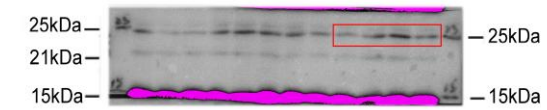


Figure 3F T-AMPK 62kDa

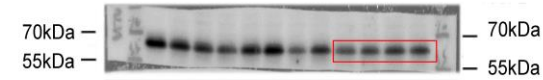


Figure 3G β-Actin 43kDa

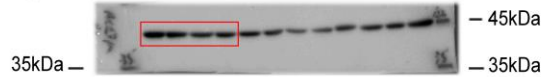
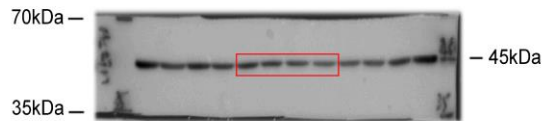


Figure 3F β-Actin 43kDa



Supplement figure 5.

Figure 4A P-ERK1/2^{T202/Y204} 44, 42kDa

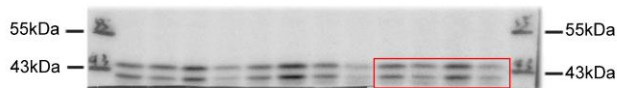


Figure 4B P-nNOS^{S1417} 165kDa

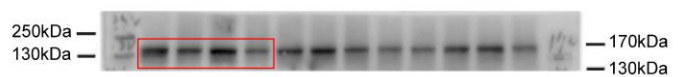


Figure 4A T-ERK1/2 44, 42kDa

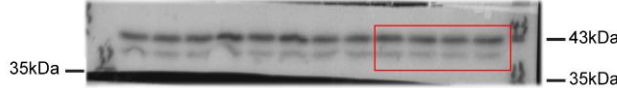


Figure 4B T-nNOS 165kDa



Figure 4A P-RSK^{T359/S363} 90kDa

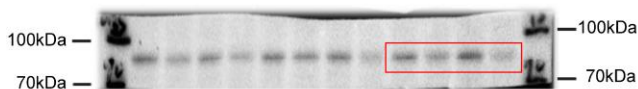


Figure 4B P-eNOS^{S1177} 140kDa

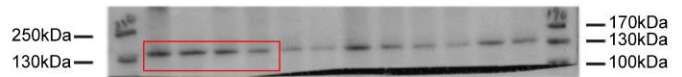


Figure 4A T-RSK 90kDa

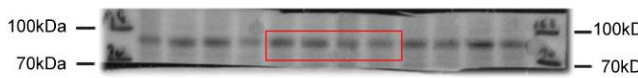


Figure 4B T-eNOS 140kDa

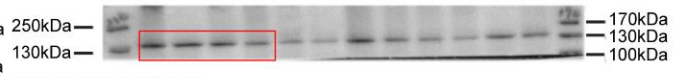


Figure 4A β-Actin 43kDa

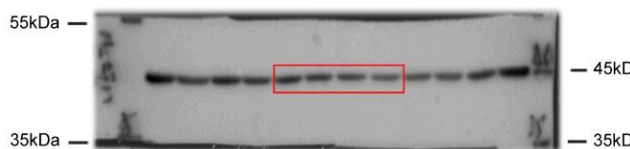


Figure 4B iNOS 130kDa



Figure 4B β-Actin 43kDa

